Broad-Band Spectra of GPS/CSS Sources

Łukasz Stawarz

(& Luisa Ostorero, Stefan Wagner, et al.)

Landessternwarte Heidelberg, Heidelberg, Germany

Max-Planck-Institut für Kernphysik, Heidelberg, Germany

Obserwatorium Astronomiczne UJ, Kraków, Poland

Radio Spectra – Examples

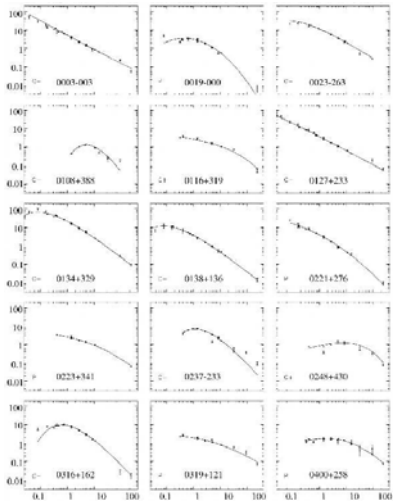

General Characteristics

'GHz Peaked Spectrum' (GPS):

- $\nu_{\rm p} \sim 0.5 - 10\,$GHz
- $LS \lesssim 1\,$kpc

'Compact Steep Spectrum' (CSS):

- $\nu_{\rm p} \lesssim 0.5\,$GHz
- $LS \sim 1 - 10\,$kpc

GPS/CSS Population:

- Nuclei of GPS and CSS objects classified as RGs, QSOs, Sy 1s, or Sy 2s.
- GPS/CSS similar to classical doubles (FR IIs) $\Rightarrow$ 'Compact Symmetric Objects' (CSOs) if $LS \lesssim 1\,$kpc, or 'Medium Symmetric Objects' (MSOs) if $LS \sim 1 - 10\,$kpc.
- GPS/CSS with a 'core–jet' morphology $\Rightarrow$ 'true' GPS/CSS objects or 'regular' radio-loud quasars viewed in projection?
- About 10% of radio sources found in high-frequeny radio surveys belongs to the GPS class, while 30% is classified as CSS objects.

$\nu_{\rm p} - LS$ Anticorrelation

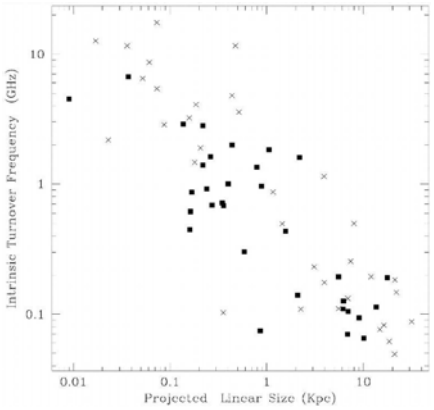

O'Dea & Baum 1997

- $\nu_{\rm p} \propto LS^{-0.65}$, however with a large scatter.
- The observed correlation implies unification of GPS and CSS populations.
- Continuous distribution up to the observationally limited $\nu_{\rm p} \sim 10\,$GHz suggests an unnoticed population of sources with $\nu_{\rm p} > 10\,$GHz ('High Frequency Peakers').
- *(Question: what does it mean if most of the sources from the sample are not realy GPS/CSS sources?)*

Radio Powers

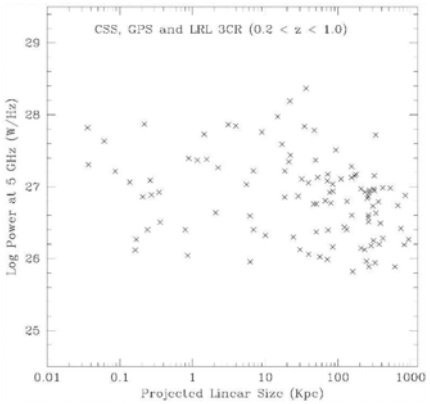

O'Dea 1998

- The 'true' GPS/CSS sources have to be *intrinsically* very powerful in radio, because Doppler and projection effects seem to be minor.
- Radio powers at 5 GHz always exceed the FR I/FR II division, $L_{5\,\mathrm{GHz}} \sim 10^{25}\,\mathrm{W\,Hz^{-1}}$, and reach $\sim 10^{29}\,\mathrm{W\,Hz^{-1}}$ in some cases.
- Since they are as powerful as classical doubles but much smaller, GPS/CSS objects can be either young version of the extended radio sources (*Phillips & Mutel 1982*) or examples of radio-loud AGNs 'frustrated' by the ambient medium (*van Breugel et al. 1984*).

Ages of GPS/CSS Sources

- Spectral ageing analysis of radio lobes gives the ages
  .
  $< 10^4$ yrs for GPS sources ($B_{\mathrm{eq}} \sim 10\,\mathrm{mG}$), and
  $\sim 10^4 - 10^5$ yrs for CSS objects ($B_{\mathrm{eq}} \sim 1\,\mathrm{mG}$),
  .
  with the injection spectral indices ranging from 0.35 up to 0.8 (*Murgia et al. 1999*).
- The spectral ages are consistent with the kinematic ages for the advanced velocities on average $v_{\mathrm{adv}} \sim 0.3c$.
- Such high advanced velocities were in fact detected in a number of GPS/CSS sources (*Gugliucci et al. 2005*). The ram-pressure arguments suggest density of the ambient medium $n_{\mathrm{e}} < 1\,\mathrm{cm^{-3}}$ (typical for the extended radio sources).
- This suuports the 'youth' scenario, and contradicts the 'frustration' scenario, since the latter requires total masses of cold ambient gas in a range $10^{10} - 10^{11}\,M_{\odot}$ within the host galaxies (which would be then similar to the amount of gas present in ultraluminous infrared galaxies, but much larger than amount of gas in hosts of other radio-loud AGNs).

Spectral Turnover

- Spectral turnover due to either synchrotron self-absorption (SSA) or free-free absorption (FFA) through a screen of dense ambient matter.
- The sources' parameters obtained by means of applying *both* models to observational data are roughly realiable and consistent with the other constraints for many particular objects, mostly due to observational limitations; problems were noted in either cases, and the general requirement in both models is an inhomogeneous structure of the absorbing medium.
- The observed spectral indices below the peak frequency are usually $\alpha_{\mathrm{low}} \geq -2$ (where the flux density is $S_\nu \propto \nu^{-\alpha}$), in some cases are bit flatter and close to the standard value $-5/2$ predicted by the homogeneous SSA model, while in the other cases are even consistent with the exponential cutoff predicted by the simplest version of the FFA model.
- The variety of the low-frequency spectral indices indicates therefore inhomogeneity of the absorbing medium, as mentioned above, and/or superposition of several emission components with different physical parameters.
- The fact that in many cases $\alpha_{\mathrm{low}} < -1/3$, i.e. that the low-frequency continua are flatter than the flattest optically thin synchrotron spectrum which can be produced, indicates that some absorption has to be present.

Template Radio Spectrum (?)

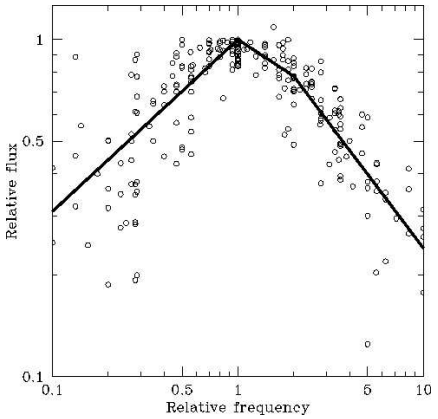

De Vries et al. 1997

- The average spectral indices for the analyzed sample of GPS/CSS sources are $\alpha_{\mathrm{low}} = -0.51(\pm 0.03)$ and $\alpha_{\mathrm{high}} = +0.73(\pm 0.06)$ below and above the peak frequency, respectively.
- The values of α_{high} are characterized by a very broad distribution between $+0.5$ and $+1.2$.
- There may be also a flat spectral plateau between ν_{p} and $2 \times \nu_{\mathrm{p}}$ in the template GPS/CSS spectrum, with average power-law slope $\alpha_{\mathrm{flat}} = +0.36(\pm 0.05)$.

Ambient Medium

- In many objects there are strong evidences for the FFA due to nuclear disk/torus-like structure of the obscuring material with < 100 pc size and $N_{\rm H}$ up to $\sim 10^{23}$ cm^{-2} (*Peck et al. 1999, Kameno et al. 2000, Marr et al. 2001, Mutoh et al. 2002, Kameno et al. 2003*).
- GPS sources exhibit (very) low polarization of their radio fluxes ($few\%$, if any), while radio continua of CSS objects a bit higher. This is most likely due to Faraday depolarisation. The observed RM has a very broad scatter in the GPS/CSS sample, from very large, $RM \sim 10^4$ rad m^{-2}, to very small, $RM \lesssim 10^2$ rad m^{-2}. Faraday screen seems to be associated with the optical line-emitting clouds interacting with jets (*Cotton et al. 2003, 2006*).
- Very broad HI absorption lines are often detected in GPS/CSS objects (at much higher rate than in extended radio galaxies), with the hydrogen column densities (anticorrelating with the sources' sizes) in a range between $N_{\rm H} \sim 10^{22}$ cm^{-2} down to $N_{\rm H} \sim 10^{19}$ cm^{-2} *Vermeulen et al. 2003, Pihlström et al. 2003, Gupta et al. 2006*). Detailed studies of a few objects indicate that the HI absorption lines are well associated with optical emission lines, and thus arise most likely in the atomic cores of Narrow Line Region (NLR) clouds distributed within ~ 1 kpc radius around active nuclei, and interacting with the expanding radio source (*Labiano et al. 2006, Vermeulen et al. 2006*).

Infrared-To-Optical

- GPS/CSS sources have the same MFIR strenghts as extended sources with comparale radio powers and redshifts, i.e., $\langle L_{50\,\mu{\rm m}} \rangle \sim 3 \times 10^{45}$ erg s^{-1} for $\langle L_{5\,{\rm GHz}} \rangle \sim 10^{44}$ erg s^{-1} in the case of GPS/CSS radio galaxies (*Heckman et al. 1994, Hes et al. 1995, Fanti et al. 2000*).
- Host galaxies of GPS/CSS sources are very similar to host galaxies of powerful (3CR) classical doubles when observed in NIR, being evolved ellipticals with some morphological indications of relatively recent merger events (*De Vries et al. 1998, 2000*). Very often they exhibit also kpc-scale optical emission aligned with the main axis of radio source, with line luminosities of about $L_{\rm opt}^{\rm ext} \sim 10^{42} - 10^{43}$ erg s^{-1}, and outflow velocities of $v_{\rm out} \sim 10^8$ cm s^{-1} (*De Vries et al. 1999, Axon et al. 2000, O'Dea et al. 2002, Labiano et al. 2005*).
- At near UV frequencies, GPS/CSS sources, similarly to classical doubles, exhibit complex spectra composed from nebular continuum, nuclear light, and starburst component *(Tadhunter et al. 2002*). GPS/CSS quasars possess often acrretion disk-related UV-bumps, with the luminosities of $L_{\rm UV} \geq 10^{46}$ erg s^{-1}, the value characteristic for powerful quasars in general.

Dusty Tori

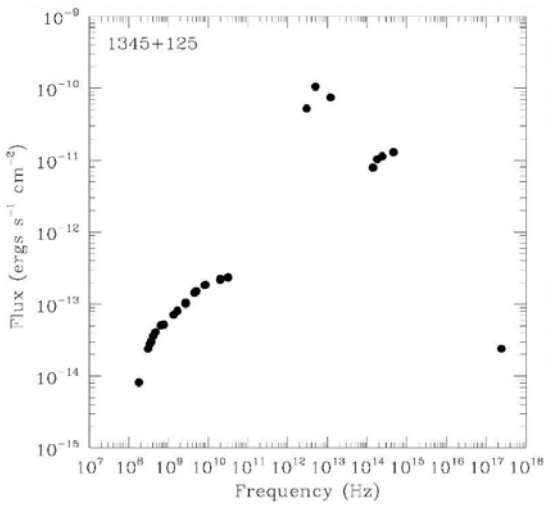

X-rays

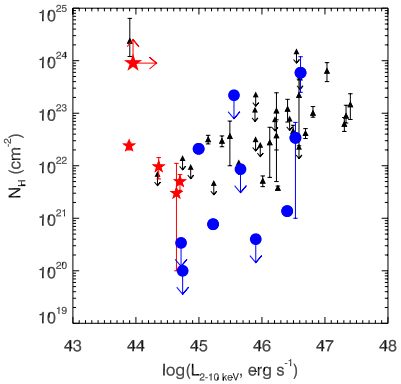

Guainazzi et al. 2006: GPS galaxies (stars), GPS/CSS quasars (circles), RL QSOs (triangles).

- X-ray observations show that GPS/CSS sources are heavily obscured rather than intrinsically weak in X-rays (*Guainazzi et al. 2006, Vink et al. 2006, Siemiginowska et al. 2006*).
- The X-ray obscuration is consistent with the presence of obscuring nuclear tori, just like in the case of extended and powerful radio-loud AGNs: $N_{\rm H}$ ranges from $\sim 10^{21}$ cm^{-2} up to $\geq 10^{23}$ cm^{-2}.
- In some cases excess hard X-ray emission reported (CSS objects 3C 48, PKS 2004-447, and 3C 303.1; *Worrall et al. 2004, Gallo et al. 2006, O'Dea et al. 2006*).

X-ray Spectra – Examples

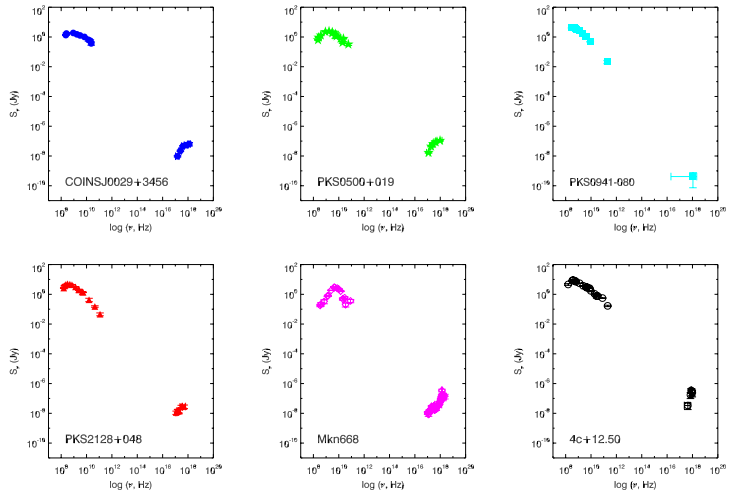

They are young! (And SSA-ed ?)

- 'Youth' scenarios differ in the
  assumed profiles for the ambient medium density, $\rho(r)$,
  assumed self-similar/non self-similar lobes' evolution,
  assumed constant jet power/jet intermittency
  (see *Phillips & Mutel 1982, Carvalho 1985, Fanti et al. 1995, Readhead et al. 1996, Begelman 1996, Reynolds & Begelman 1997, Alexander 2000, Snellen et al. 2000, Perucho & Marti 2002, Kawakatu & Kino 2006*).
- Therefore, evolution of the sources' parameters (radio luminosity, hotspots' velocities, etc) are different in different models.
- Usually, the youth scenarios associate spectral turnover to the SSA process, although such an association is not required.
- The evolutionary models with spectral turnover due to SSA cannot explain *easily* the observed $\nu_{\rm p} - LS$ anticorrelation.

Not Frustrated! Although Obscured, Depolarized (and FFA-ed ?)

- A number of authors interpreted small sizes of GPS/CSS sources in terms of an efficient confinement of expanding radio structure by dense galactic environment, associated in a natural way with NLR (*van Breugel et al. 1984, Gopal-Krishna & Wiita 1991*).
- This interpretation was believed to explain nicely at the same time the characteristic for the GPS/CSS class spectral turnover and neglegible radio polarisation, as results of FFA and Faraday rotation/depolarisation, respectively, on clumpy NLR screen surrounding the discussed radio structures.
- However, since GPS/CSS objects are as powerful in radio as classical doubles, the postulated confinement requires the environment much denser than described above. Such significantly denser environments of GPS/CSS sources were indeed claimed previously, but are not supported by the most recent multiwavelength studies.
- On the other hand, GPS/CSS sources do interact strongly with the clumpy/multi-phase ambient medium, are heavily obscured and depolarized, and so can be indeed FFA-ed (*De Young 1993, 1997, Bicknell et al. 1997, Carvalho 1994, 1998*).
- Still, the FFA absorption models cannot explain *easily* the observed $\nu_{\rm p} - LS$ anticorrelation (but see *Bicknell et al. 1997*).

Cocoon's Evolution

All the models describing evolution of GPS/CSS sources start from the set of equations introduced by *Begelman & Cioffi (1989)*:

$$L_{\rm j} = c\,\rho(LS)\,v_{\rm h}^2\,A_{\rm h} \quad , \quad p = \rho(l_{\rm c})\,v_{\rm c}^2 \quad , \quad 3\,p\,V = 2\,L_{\rm j}\,t \quad ,$$
$$v_{\rm h} = \frac{d\,LS}{dt} \quad , \quad v_{\rm c} = \frac{d\,l_{\rm c}}{dt} \quad , \quad \frac{d\,V}{dt} = 2\pi\,l_{\rm c}^2\,v_{\rm h} \quad . \qquad (1)$$

For the given jet power $L_{\rm j}$ and ambient medium density profile $\rho(r)$, as well as for the parameter of choice LS, the number of variables is larger than the number of equations (1). To close the system, we follow *Kawakatu & Kino (2006)*, who introduced a general scalling

$$l_{\rm c}^2 \propto t^X \quad . \qquad (2)$$

In addition, we restrict our analysis to young GPS/CSS sources, which evolve in a central plateau of the galactic gaseous halo, and which are young $t \leq 10^5$ yr. Thus, we set the ambient density profile as $\rho = m_{\rm p}\,n_0$ with the expected $n_0 \sim 0.1\,{\rm cm}^{-3}$, and fix $X = 1$ to reproduce the appropriate *'1D'* jet evolution found in the numerical analysis of *Scheck et al. (2002)*. Such a choice gives $v_{\rm h} \propto LS^0$ (as required by observations), $v_{\rm c} \propto LS^{-1/2}$, $p \propto LS^{-1}$, $l_{\rm c} \propto LS^{1/2}$, $V \propto LS^2$, $t \propto LS$, and $A_{\rm h} \propto LS^0$.

Cartoon by *Kino & Kawakatu (2006)*

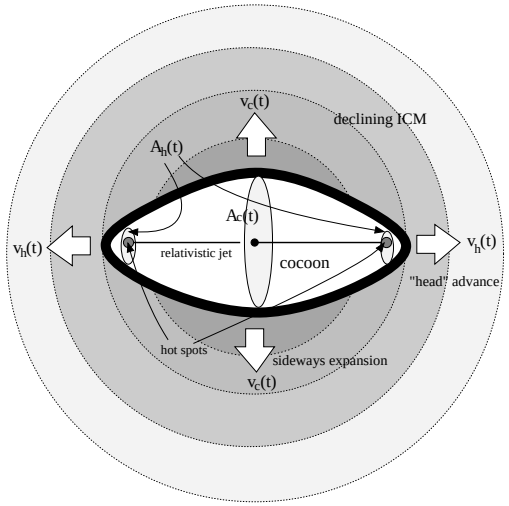

Cocoons' Magnetic Field

We assume that the cocoons of GPS/CSS objects, just like cocoons of extended powerful radio sources, are close to the minimum power condition. In general, one can parameterize magnetic field energy density in the cocoon as $U_{\rm B} = \eta\, p$, with $\eta \leq 1$. For example, in the case of energy equipartition between the lobe's ultrarelativistic electrons, ultrarelativistic protons and magnetic field, one has $\eta = 1$. Thus,

(3) $$U_{\rm B} = \eta \left(\frac{L_{\rm j}\, m_{\rm p} n_0\, v_{\rm h}}{6\pi} \right)^{1/2} LS^{-1} \approx 10^{-4}\, \eta\, L_{\rm j,\,45}^{1/2}\, n_{-1}^{1/2}\, \beta_{0.3}^{1/2}\, LS_1^{-1} \quad {\rm erg\,cm^{-3}} \quad ,$$

where $L_{\rm j,\,45} \equiv L_{\rm j}/10^{45}\,{\rm erg\,s^{-1}}$, $n_{-1} \equiv n_0/0.1\,{\rm cm^{-3}}$, $\beta_{0.3} \equiv v_{\rm h}/0.3\,c$, and $LS_1 \equiv LS/1\,{\rm pc}$. This, with the expected $n_{-1},\ \beta_{0.3} \sim 1$, gives the cocoon's magnetic field intensity

(4) $$B = (8\pi\, U_{\rm B})^{1/2} \approx 0.05\, \eta^{1/2}\, L_{\rm j,\,45}^{1/4}\, LS_1^{-1/2} \quad {\rm G} \quad .$$

For $L_{\rm j,\,45} \geq 1$ and $\eta \sim 1$ one therefore obtains $B \sim 10\,{\rm mG}$ and $B \sim 1\,{\rm mG}$ for the GPS ($LS \sim 0.01 - 1\,{\rm kpc}$) and CSS ($LS \sim 1 - 10\,{\rm kpc}$) objects, respectively, consistently with observational constraints.

Scaling Laws

Assuming that the terminal shock injects power-law electron energy distribution $N_{\rm e}(\gamma) = N_0\, \gamma^{-s}$ (with *fixed spectral shape*) to the expanding lobe, and that $U_{\rm e} \propto U_{\rm B}$ (with $U_{\rm B}$ as given above), one can find the bolometric synchrotron luminosity

(5) $$L_{\rm syn} \propto U_{\rm B}\, U_{\rm e}\, V \propto LS^0$$

The monochromatic synchrotron power measured at some fixed observed frequency $\nu^\star$ (and thus produced by the electrons with different eneregies at different times of observation, because of a change in the magnetic field intensity) scales as

(6) $$[\nu^\star L_{\nu^\star}] \propto B^{(s-3)/2}\, U_{\rm B}\, U_{\rm e}\, V \propto LS^{(3-s)/4}$$

The characteristic SSA frequency scales as

(7) $$\nu_{\rm ssa} \propto LS^{-x} \quad {\rm with} \quad x = (s+2)/(2s+8) = 0.3 - 0.36$$

for $s = 1 - 3$, while the observed power at such SSA frequency scales as

(8) $$[\nu_{\rm ssa} L_{\nu_{\rm ssa}}] \propto B^{(s-3)/2}\, \nu_{\rm ssa}^{(3-s)/2}\, U_{\rm B}\, U_{\rm e}\, V \propto LS^{y} \quad {\rm with} \quad y = (3-s)/(2s+8) = 0.2 - 0$$

Intrinsic Turnover?

The electrons can undergo 1st order Fermi acceleration at the jet terminal (reverse) shock if they are able to be scattered by the turbulence at both sides of the shock front. In the case of the cold protons carrying bulk of the kinetic energy of powerful jets on large ($>$ pc) scales the maximum frequency of the Alfv'enic turbulence is set by the cold proton gyrofrequency $\Omega_{\rm p}$. This implies that the electrons which can undergo 1st order Fermi acceleration at the jet head have to be already ultrarelativistic. Indeed, taking the appropriate resonance condition for the electron–Alfvén wave interaction $\lambda \sim r_{\rm e}$, where λ is the wavelength of a turbulent mode and $r_{\rm e} = \gamma\, m_{\rm e} c^2/e\, B_{\rm HS}$ is the electron gyroradius for the hotspot magnetic field $B_{\rm HS}$, together with the dispertion relation for the non-compressive Alfvén waves $\omega^2 = v_{\rm A}^2\, k^2$, where $k = 2\pi/\lambda$, $v_{\rm A} = \beta_{\rm A}\, c$ is the Alfvén velocity, and $\omega < \Omega_{\rm p}$, one obtains (see *Bell 1978*)

(9) $$\gamma_{\rm cr} \approx \beta_{\rm A}\, \Gamma_{\rm j}\, \frac{m_{\rm p}}{m_{\rm e}}$$

In the above, we put the cold protons' gyrofrequency $\Omega_{\rm p} = e\, B_{\rm HS}/\Gamma_{\rm j}\, m_{\rm p} c$, where $\Gamma_{\rm j}$ is the jet bulk Lorentz factor, since the cold protons carrying bulk of the jet kinetic energy are shocked at the jet head to the average energy $\Gamma_{\rm j}\, m_{\rm p} c^2$ (assuming only mildly-relativistic advance velocity of the hotspot itself).

Turnover Frequency

Is it therefore possible that the turnover frequency observed in GPS/CSS sources is due to the electrons with Lorentz factors $\gamma_{\rm cr}$? With the magnetic field intensity as given previously, this frequency would read as

(10) $$\nu_{\rm p} = \frac{e\,B\,\gamma_{\rm cr}^2}{4\pi\,m_{\rm e}c} \approx 60\,\beta_{\rm A,\,-1}^2\,\Gamma_{\rm j,\,5}^2\,\eta^{1/2}\,L_{\rm j,\,45}^{1/4}\,LS_1^{-1/2} \quad {\rm GHz} \quad ,$$

where $\Gamma_{\rm j,\,5} \equiv \Gamma_{\rm j}/5$ and $\beta_{\rm A,\,-1} \equiv \beta_{\rm A}/0.1$.

.

Note three important features in the above formula:

- values of $\nu_{\rm p}(LS)$ as required;
- weak dependance on $L_{\rm j}$;
- anticorrelation $\nu_{\rm p} \propto LS^{-0.5}$ *almost* as the observed one $\nu_{\rm p} \propto LS^{-0.65}$.

.

If, in addition, $\Gamma_{\rm j} \propto LS^{-0.065}$....

What About the 'Classical' Hotspots?

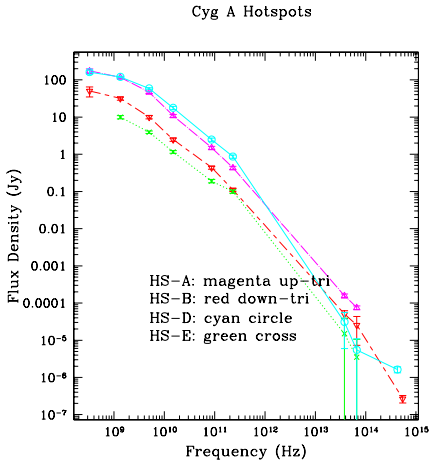

Spectral turnover for $\gamma_{\rm cr} \sim 10^3$ is indeed the case! (*Carilli et al. 1991, Harris et al. 2006*).

How to Check It?

In the case of powerful radio sources infrared emission of dusty tori is likely to dominate the other photon fields on scales between 1 pc and 1 kpc. Energy density of this emission at the distance r from the galactic center can be estimated as

(11) $$U_{\rm IR} = \frac{L_{\rm IR}}{4\pi\,c\,r_{\rm d}^2}\,\frac{1}{1+(r/r_{\rm d})^2} \quad ,$$

where $L_{\rm IR}$ is the torus luminosity (which is typicaly some small ζ fractions of the accretion-related UV luminosity of the active center, $L_{\rm IR} \sim \zeta\,L_{\rm UV}$), and $r_{\rm d} = (L_{\rm UV}/4\pi\,\sigma_{\rm SB}\,T_{\rm d}^4)^{1/2}$ is the characteristic scale of the torus with the temperature $T_{\rm d}$ (*Sikora et al. 2002, Błażejowski et al. 2000, 2004*). For powerful quasars $L_{\rm UV} \sim 10^{46} - 10^{47}\,{\rm erg\,s^{-1}}$, $\zeta \sim 0.1$, and $T_{\rm d} \sim 10^3$ K, what is consistent with the typical MFIR emission observed from GPS/CSS sources. Since $r_{\rm min}$ is expected to be much smaller than the distances considered here,

(12) $$r_{\rm d} \sim L_{\rm IR,\,45}^{1/2}\,\zeta_{-1}^{-1/2}\,T_3^{-2} \quad {\rm pc} \quad ,$$

where $L_{\rm IR,\,45} \equiv L_{\rm IR}/10^{45}\,{\rm erg\,s^{-1}}$, $\zeta_{-1} \equiv \zeta/0.1$, and $T_3 \equiv T_{\rm d}/10^3$ K, one can restrict the analysis to $LS > r_{\rm d}$, obtaining $U_{\rm IR}(LS > r_{\rm d}) \sim 3 \times 10^{-4}\,L_{\rm IR,\,45}\,LS_1^{-2}\,{\rm erg\,cm^{-3}}$.

Comptonisation of the IR Torus Emission

Emission due to comptonisation of the IR photons produced by the dusty torus within the radio cocoon is expected to peak at the characteristic frequency

(13) $$\varepsilon_{\rm ic,\,cr} = \varepsilon_{\rm IR}\,\gamma_{\rm cr}^2 \sim 100\,\beta_{\rm A,\,-1}^2\,\Gamma_{\rm j,\,5}^2 \quad {\rm keV} \quad ,$$

with the luminosity

(14) $$L_{100\,{\rm keV}} \sim \frac{U_{\rm IR}}{U_{\rm B}}\,L_{\rm p} \quad .$$

Such an emission can be strong enough to be detected by SWIFT/SUZAKU, since

(15) $$\frac{U_{\rm IR}}{U_{\rm B}} \sim 3 \times L_{\rm IR,\,45}\,\eta^{-1}\,\xi_{-1}^{1/2}\,L_{\rm p,\,44}^{-1/2}\,LS_1^{-1} \quad ,$$

where we have introduced the efficiency factor in converting jet power to the radio (peak) luminosity of the cocoon, $\xi \equiv L_{\rm p}/L_{\rm j}$, and put $\xi_{-1} \equiv \xi/0.1$, $L_{\rm p,\,44} \equiv L_{\rm p}/10^{44}\,{\rm erg\,s^{-1}}$. Note, that for the observed $\langle L_{\rm IR,\,45}\rangle \sim 3$ and $\langle L_{\rm p,\,44}\rangle \sim 1$, and the expected GPS/CSS parameters η, $\xi_{-1} \sim 1$, this reads as $\langle U_{\rm IR}/U_{\rm B}\rangle \sim 10\,LS_1^{-1}$.

To Conclude:

Single power-law spectra of ultrarelativistic electrons is just a zero-order approximation.

.

for example 3C 273 jet:

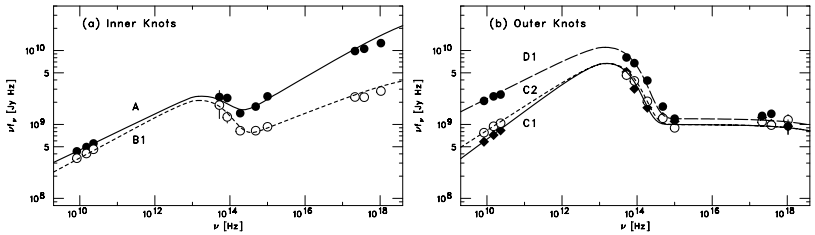

(*Uchiyama et al., 2006*)